Supporting Information

Deciphering Multiple Energy-transfer Photoevents in a 2D-MOF Composite: Relevance to Multicolor Lighting

Samita Mishra[†], Jordi Torró-Abril[‡], Urbano Díaz[‡], Boiko Cohen[†], and Abderrazzak Douhal[†*]*

†Departamento de Química Física, Facultad de Ciencias Ambientales y Bioquímica, and INAMOL, Universidad de Castilla-La Mancha, Avenida Carlos III, S/N, 45071 Toledo, Spain.

‡Instituto de Tecnología Química, Universitat Politécnica de Valéncia-Consejo Superior de Investigaciones Científicas (UPV-CSIC), Av. de los Naranjos s/n, 46022 Valencia, Spain.

Corresponding Authors:

E-mail: Abderrazzak.Douhal@uclm.es Phone: +34-925-265717 (A.D.).

E-mail: Boiko.Cohen@uclm.es

Table of Contents

S.N.	Figure/Table	detail
1		Materials and synthesis of Al-ITQ-HB, C153@Al-ITQ-HB and C153/NR@M-ITQ-HB.
2		Morphology, Spectroscopic and Dynamic Measurements.
3	Figure S1	A) Images of the composites under daylight and UV light; B) TEM images of the Al-ITQ-HB, the C153@ Al-ITQ-HB composite and C153/NR@ Al-ITQ-HB mixed composite.
4	Figure S2	A) Absorption spectra of solid C153 and C153@Al-ITQ-HB composites with different initial concentrations; B) Emission spectra of solid dye and 10^{-6} M C153 in DCM; C) Emission spectra of different $[C153]_0$ at Al-ITQ-HB upon excitation at 425 nm. 10^{-6} M (blue), 10^{-5} M (green), 10^{-4} M (orange); 10^{-3} M (red) and 10^{-2} M (brown) and solid dye (dark green).
5	Table S1	Steady state data of C153@Al-ITQ-HB.
6	Figure S3	Absorption, emission (following excitation at 425 nm) and excitation (collected at 525 nm emission) spectra of different $[C153]_0$ composites.
7	Figure S4	Emission decays of C153@Al-ITQ-HB composites collected at discrete wavelengths following excitation at 433 nm.
8	Table S2	Fit parameters for the C153 composites following excitation at 433 nm, 10^{-6} M $[C153]_0$.
9	Table S3	Fit parameters for the C153 composites following excitation at 433 nm. A) 10^{-4} M; B) 10^{-2} M $[C153]_0$.
10	Figure S5	Spectral overlaps between absorption (NR) and emission (C153) spectra in the mixed composites.
11	Figure S6	Absorption, emission (excitation at 425 nm), excitation (emission at C153 maxima) and excitation (emission at NR maxima) spectra of the C153/NR@ Al-ITQ-HB mixed composites
12		Energy transfer efficiency (ET) calculation.
13	Figure S7	Emission decays of Group 1 and Group 2 [NR/C153@Al-ITQ-HB] composites collected at discrete wavelengths following excitation at 505 nm.
14	Figure S8	Emission decays of [NR/C153@Al-ITQ-HB] composites collected at discrete wavelengths following excitation at 505 nm. A) $[C153/NR: 10^{-5}$ M/10^{-4} M$]_0$; B) $[C153/NR: 10^{-4}$ M/10^{-5} M$]_0$.
15	Figure S9	Emission decays of NR@Al-ITQ-HB composites collected at discrete wavelengths following excitation at 505 nm. A)

		10^{-4} M and B) 10^{-5} M $[NR]_0$.
16	Table S4	Fit parameters for the emission decays obtained after 505 nm excitation. A) [C153/NR: 10^{-3} M/10^{-4} M]$_0$; B) [C153/NR: 10^{-4} M/10^{-4} M]$_0$.
17	Table S5	Fit parameters for the emission decays collected after 505 nm excitation. A) [C153/NR: 10^{-5} M/10^{-4} M]$_0$; B) [C153/NR: 10^{-5} M/10^{-5} M]$_0$
18	Table S6	Fit parameters for the emission decays of NR composites obtained after 505 nm excitation. A) 10^{-4} M and B) 10^{-5} M $[NR]_0$.
19	Table S7	Fit parameters for the emission decays obtained after 505 nm excitation. A) [C153/NR: 10^{-3}/10^{-5} M]$_0$; B) [C153/NR: 10^{-4} M/10^{-5} M]$_0$.
20		Synthesis of the composites to study the effect of preparation method on hetero-ET.

Materials and synthesis of Al-ITQ-HB, C153@Al-ITQ-HB and C153/NR@Al-ITQ-HB. The Al-ITQ-HB MOF was synthesized using reported method.[1] The Al-ITQ-HB material was prepared by dissolving equimolar amounts of $AlCl_3 \cdot 6H_2O$ (3.1 mmol) and HB acid (3.1 mmol) in two separate portions of dimethylformamide (DMF, 15 mL each). These two solutions were then combined, and the resulting mixture was transferred into a stainless-steel autoclave. The sealed vessel was heated at 150 °C for 24 hours under autogenous pressure and static conditions. After cooling to room temperature, the solid product was recovered by filtration, followed by thorough washing with distilled water. To remove any remaining unreacted linker and DMF, the solid was stirred in methanol for 24 hours. The final material was obtained by drying the powder under vacuum at room temperature. Thereafter, we prepared the required solutions with concentrations of C153 (10^{-2}, 10^{-3}, 10^{-4}, 10^{-5}, and 10^{-6} M) and NR (10^{-4} and 10^{-5}M) in dichloromethane. To synthesize C153@Al-ITQ-HB, we added 2 mL of the C153 solution with the desired concentration to 50 mg of Al-ITQ-HB MOF and stirred the mixture for 24 hours.[2] The solvent was then removed by slow evaporation at ambient conditions obtaining the composites. To prepare the mixed composites with C153 and NR, we added 2 mL of the required concentration of each dye to 50 mg of Al-ITQ-HB, stirred the mixture for 24 hours, and evaporated the solvent. **Figure S1A** shows the images of the composites under daylight and UV light.

Morphology, Spectroscopic and Dynamic Measurements. The morphology of Al−ITQ-HB MOF, C153@Al−ITQ-HB, and [C153/NR@Al−ITQ-HB] was examined using transmission electron microscopy (TEM) with a JEOL JEM-2100F microscope operating at 200 keV. The images confirmed the mesoscopic nature of the hybrid material and demonstrated that dye loading does not alter the morphology of the Al−ITQ-HB framework (**Figure S1B**). Diffuse reflectance spectra were recorded with JASCO V-670

spectrometer with 60 mm integrating sphere (ISN-723) and corrected with the Kubelka Munk function. Fluorescence spectral measurements were performed with FluoroMax-4 (Jobin-Yvon) spectrophotometer. The fluorescence quantum yield (Q_y) of C153 composites (Q_D) and [C153/NR] composites, carried out using a Quanta-ϕ integrating sphere (Horiba) connected to FluoroMax-4 (Jobin-Yvone) spectrophotometer. Pico second time resolved emission spectra were recorded using a time-correlated single photon counting (TCSPC) setup, detailed description has given elsewhere.[3] To excite the samples, laser diodes (PicoQuant) centered at 433 and 505 nm were used with repetition rates of 40 MHz. The instrument response function (IRF) of each laser diode is ~70 ps. The fluorescence signal was controlled at magic angle (54.7) and monitored at 90^o angle with respect to the excitation source to discrete emission wavelength. To obtain the time components corresponding to the decays, single and global fits were performed using the FLUOFIT package (PicoQuant) software. The decays were deconvoluted to IRF and fitted with multiexponential functions available in the FLUOFIT package (PicoQuant). The quality of the fit was determined by the reduced value of χ^2 and the residual distribution. Fluorescence lifetime imaging microscopy (FLIM) images and decays were recorded with a MicroTime 200 microscope (PicoQuant) previously described.[4] A 390-nm pulsed diode laser (PicoQuant) was used as the excitation source at 10 MHz repetition rate and power of ~0.7 μW. The images were processed using SymPhoTime 64 software (PicoQuant). The FLIM images and the emission decays were spectrally filtered using two band-pass filters (Semrock Optical Filters), FF01-503_40-25 (D1) and FF01-650_54-25 (D2).

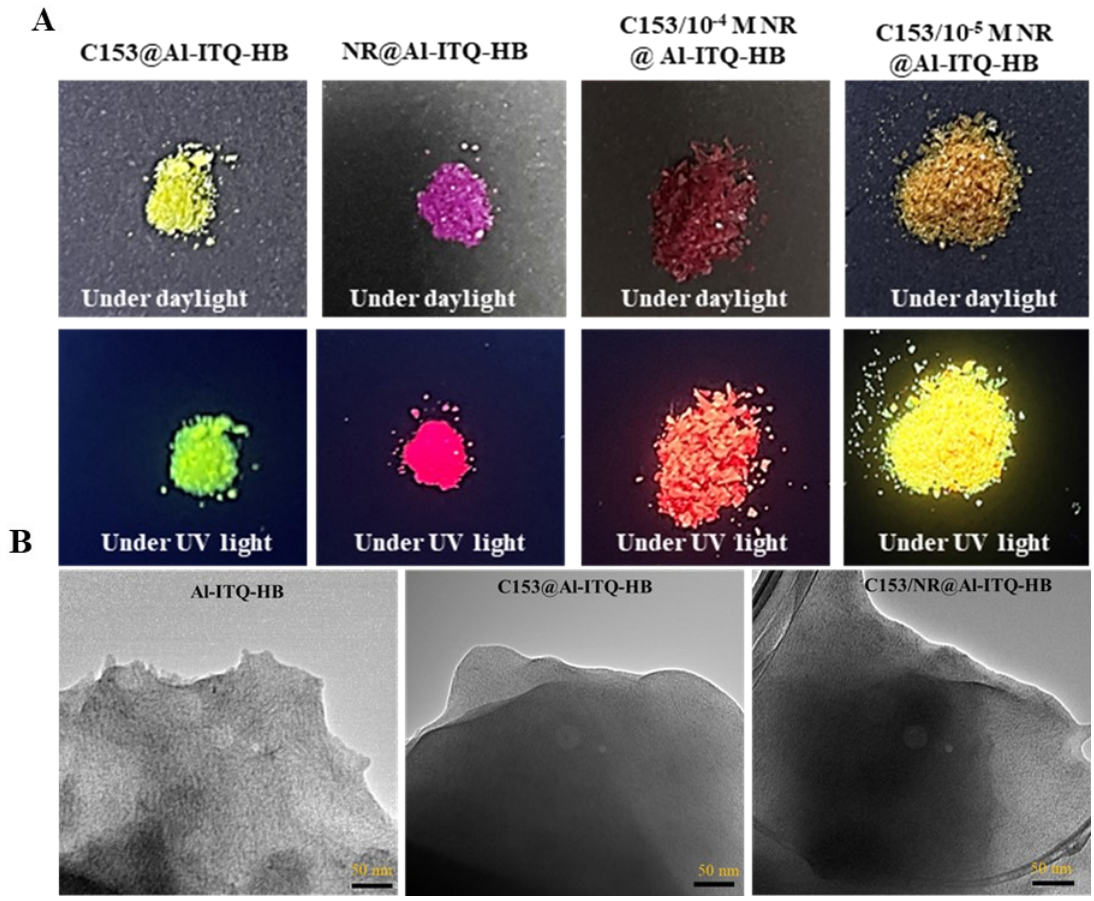

Figure S1. A) Images of the composites under daylight and UV light; B) TEM images of the Al-ITQ-HB, the C153@ Al-ITQ-HB composite and C153/NR@ Al-ITQ-HB mixed composite.

Transmission electron microscopy (TEM) analysis revealed the presence of a mesoscopically ordered structure, with mesopores clearly visible and aligned along thin, plate-like crystal domains. The images also displayed regions composed of short, stacked nanosheets, suggesting the coexistence of both lamellar and mesoporous features in the Al-ITQ-HB material. This dual character is likely associated with metal-organic nanolayers organized around disordered mesocavities. Nonetheless, the limited periodicity observed along the channels in this family of hybrid solids makes it challenging to unambiguously identify lamellar sub-domains by electron microscopy. TEM was performed on a JEOL model JEM1400Flash. For the analysis, a small amount of the sample was dispersed in dichloromethane. Then, a drop was placed on a copper grid and dried under a lamp for 2 hours.

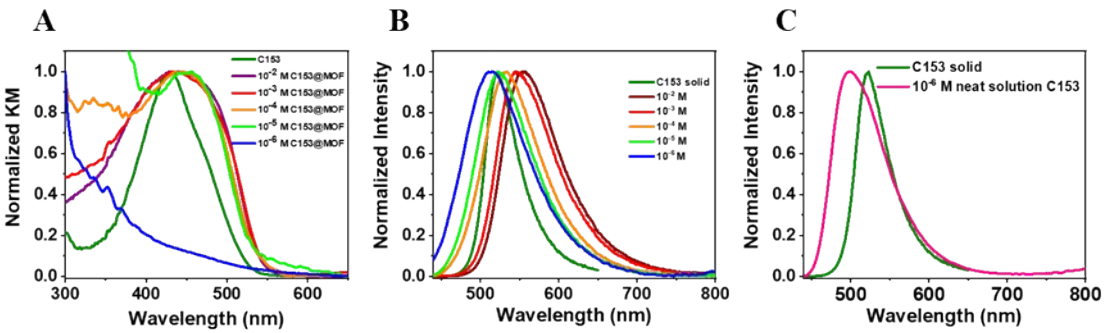

Figure S2. A) Absorption spectra of solid C153 and C153@Al-ITQ-HB composites with different initial concentrations; B) Emission spectra of solid dye and 10^{-6} M C153 in DCM; C) Emission spectra of different $[C153]_0$ at Al-ITQ-HB upon excitation at 425 nm. 10^{-6} M (blue), 10^{-5} M (green), 10^{-4} M (orange); 10^{-3} M (red) and 10^{-2} M (brown) and solid dye (dark green).

Table S1. Steady state data (Absorbance maxima, Absorbance FWHM, Emission Maxima and Emission FWHM) of C153@Al-ITQ-HB.

Sample name	Absorbance maxima (nm)	FWHM (cm^{-1})	Emission Maxima (nm)	FWHM (cm^{-1})
C153	425	5141	520	1758
10^{-6} M $[C153]_0$	-	-	516	3642
10^{-5} M $[C153]_0$	453	5590	520	3017
10^{-4} M $[C153]_0$	448	6454	533	2986
10^{-3} M $[C153]_0$	446	9210	546	2797
10^{-2} M $[C153]_0$	439	9408	556	2727

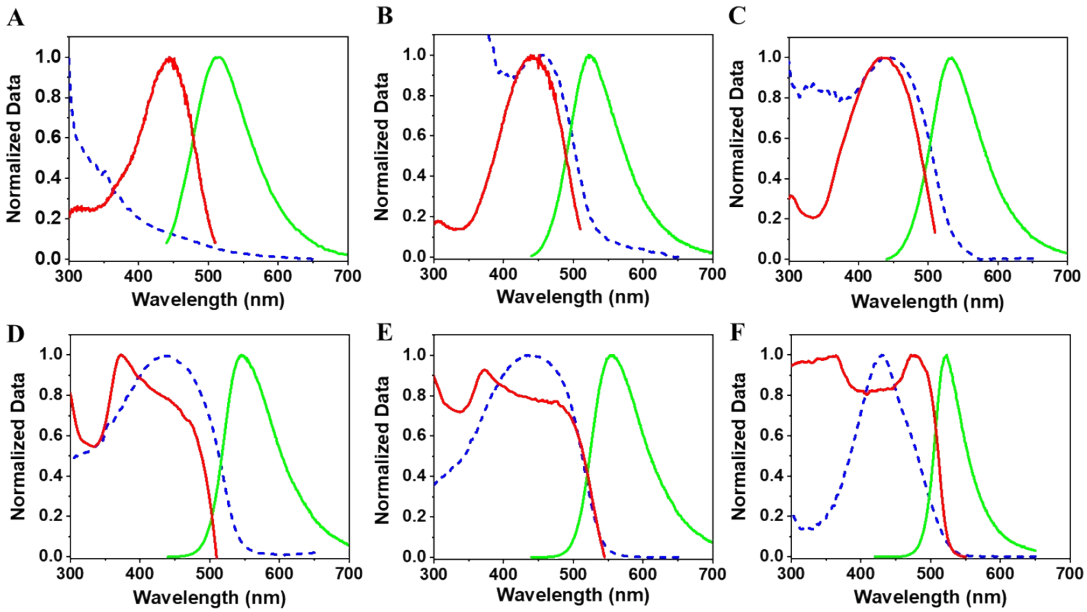

Figure S3. Absorption spectrum (blue, dashed line), emission spectrum following excitation at 425 nm (green) and excitation spectrum (red) collected at 525 nm emission of different $[C153]_0$: A) 10^{-6} M, B) 10^{-5} M, C) 10^{-4} M, D) 10^{-3} M, and E) 10^{-2} M of C153@Al-ITQ-HB composites and D) C153 solid dye.

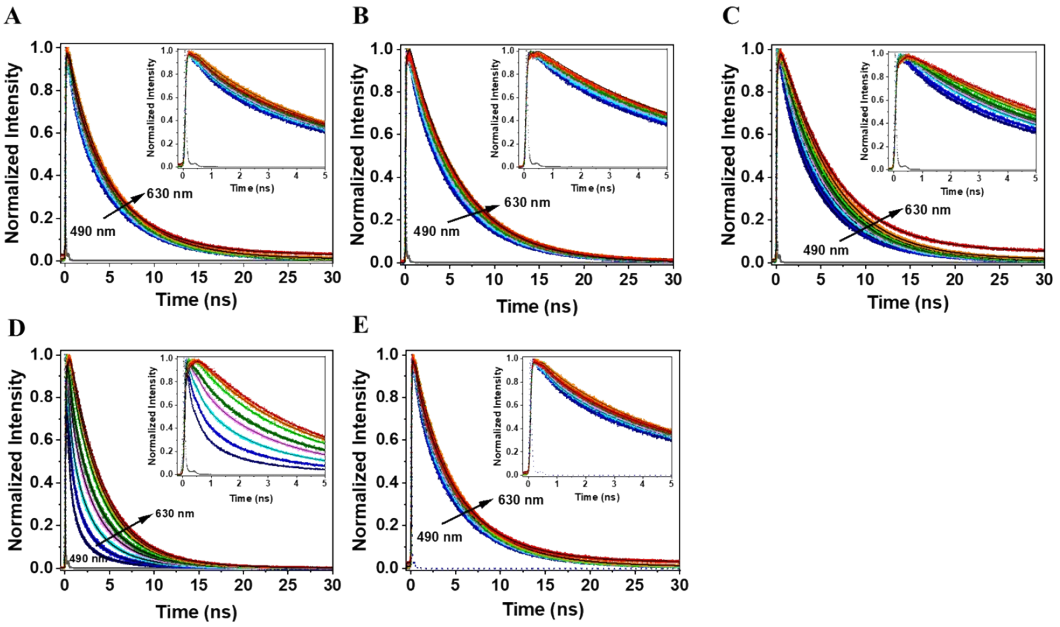

Figure S4. Emission decays (solid circles) of C153@Al-ITQ-HB composites (linear plots) collected at discrete wavelengths (490, 500, 510,520, 530, 560, 590 and 630 nm) following excitation at 433 nm. The solid black lines are the best fits of the decays using multiexponential function. The dashed line is the measured instrument response function (IRF~ 70 ps). The inset shows the zoomed scale up to 5 ns. A) 10^{-6} M; B) 10^{-5} M; C) 10^{-4} M; D) 10^{-3} M and E) 10^{-2} M $[C153]_0$.

Table S2. Values of the time components (τ_i), normalized (to 100) pre-exponential factors (A_i) and relative contributions (C_i), obtained from the multiexponential fit of the emission decays of C153@Al-ITQ-HB with 10^{-6} M $[C153]_0$, upon excitation at 433 nm.

10^{-6} M $[C153]_0$									
λ_{obs} (nm)	τ_1 (ns)	A_1 (%)	C_1 (%)	τ_2 (ns)	A_2 (%)	C_2 (%)	τ_3 (ns)	A_3 (%)	C_3 (%)
490	0.25	27	2	1.9	20	11	5.5	53	87
500	0.25	24	2	1.9	18	9	5.5	58	89
510	0.25	20	1.5	1.9	17	8.5	5.5	63	90
520	0.25	16	1	1.9	17	8	5.5	67	91
530	0.25	13	0.8	1.9	17	7.9	5.5	70	91.3
560	0.25	8	0.4	1.9	16	7.6	5.5	75	92
590	0.25	7	0.4	1.9	15	7.4	5.5	78	92.2
630	0.25	13	0.8	1.9	18	8	5.5	69	91

Table S3. Values of the time components (τ_i), normalized (to 100) pre-exponential factors (A_i) and relative contributions (C_i), obtained from the multiexponential fit of the emission decays of C153@Al-ITQ-HB with **A)** 10^{-4} M and **B)** 10^{-2} M $[C153]_0$, excitation at 433 nm.

	A) 10^{-4} M $[C153]_0$									**B) 10^{-2} M $[C153]_0$**								
λ_{obs} (nm)	**τ_1 (ns)**	**A_1 (%)**	**C_1 (%)**	**τ_2 (ns)**	**A_2 (%)**	**C_2 (%)**	**τ_3 (ns)**	**A_3 (%)**	**C_3 (%)**	**τ_1 (ns)**	**A_1 (%)**	**C_1 (%)**	**τ_2 (ns)**	**A_2 (%)**	**C_2 (%)**	**τ_3 (ns)**	**A_3 (%)**	**C_3 (%)**
490	**490**	**0.26**	**13**	**2**	**2.0**	**29**	**20**	**5.6**	**58**	**0.15**	**60**	**13**	**1.1**	**26**	**35**	**3.4**	**12**	**51**
500	**500**	**0.26**	**10**	**1**	**2.0**	**23**	**15**	**5.6**	**67**	**0.15**	**46**	**7**	**1.1**	**32**	**29**	**3.4**	**21**	**63**
510	**510**	**0.26**	**7**	**0.6**	**2.0**	**21**	**11.4**	**5.6**	**72**	**0.15**	**30**	**4**	**1.1**	**34**	**29**	**3.4**	**35**	**73**
520	**520**	**0.26**	**6**	**0.3**	**2.0**	**16**	**8**	**5.6**	**78**	**0.15**	**19**	**3**	**1.1**	**32**	**20**	**3.4**	**48**	**77**
530	**530**	**0.26**	**5**	**0.2**	**2.0**	**14**	**7**	**5.6**	**81**	**0.15**	**26**	**2**	**1.1**	**31**	**18**	**3.4**	**43**	**80**
560	**560**	**0.4**	**-100**	**-100**	**2.0**	**10**	**5**	**5.6**	**90**	**0.2**	**-100**	**-100**	**1.1**	**39**	**14**	**3.4**	**61**	**86**
590	**590**	**0.4**	**-100**	**-100**	**2.0**	**2**	**1.3**	**5.6**	**98**	**0.2**	**-100**	**-100**	**1.1**	**14**	**5**	**3.4**	**86**	**98**
630	**630**	**0.4**	**-100**	**-100**	**2.0**	**1**	**0.9**	**5.6**	**99**	**0.2**	**-100**	**-100**	**1.1**	**3**	**20**	**3.4**	**92**	**97**

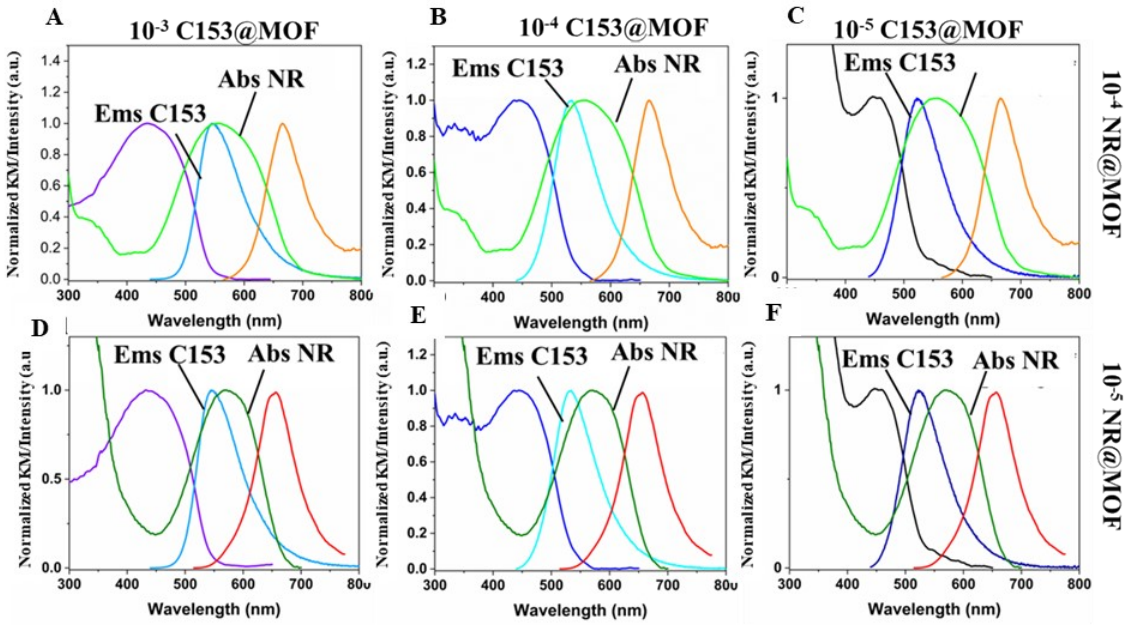

Figure S5. Spectral overlap between absorption (NR) and emission (C153) spectra in the mixed composites, *First row* **(A-C)**, 10^{-4} M $[NR]_0$ composites compared with **A)** 10^{-3} M $[C153]_0$ composites; **B)** 10^{-4} M $[C153]_0$ Composites; **C)** 10^{-5} M $[C153]_0$ composites; *second row* **(D-F)**, 10^{-5} M $[NR]_0$ composites compared with **D)** 10^{-3} M $[C153]_0$ composites; **E)** 10^{-4} M $[C153]_0$ composites; **F)** 10^{-5} M $[C153]_0$ composites. (purple, blue and black – absorption spectra of C153 composites; orange and red emission spectra of NR composites).

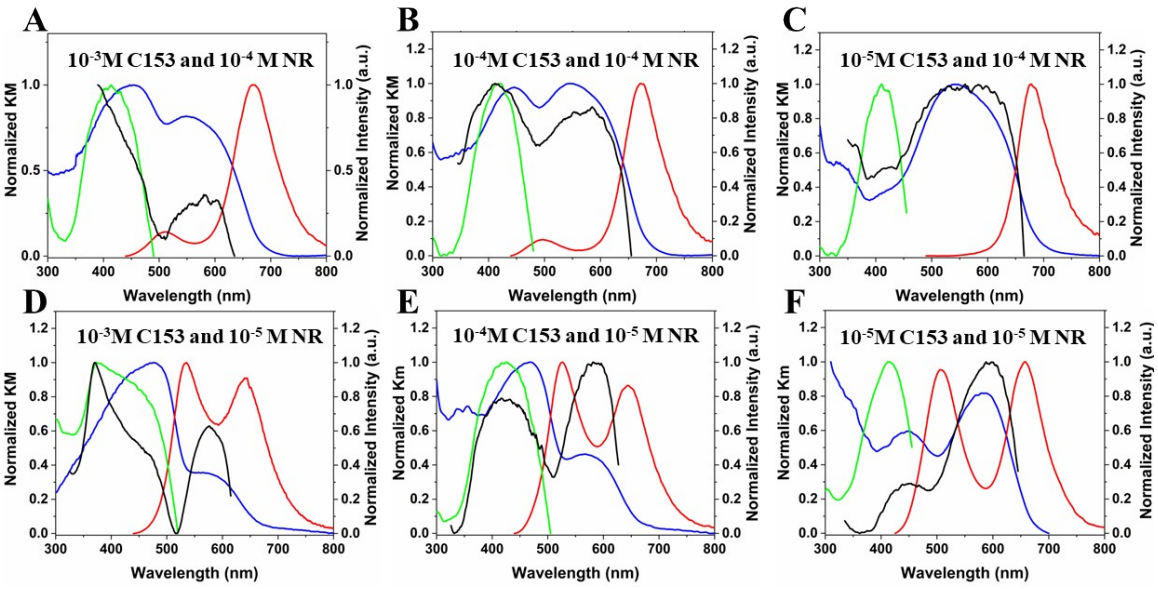

Figure S6. UV-vis absorption and emission (excitation at 425 nm) spectra of the [C153/NR@Al-ITQ-HB] (mixed) composites. *First row* **(A-C)**, Group1 composites, A) [C153/NR: 10^{-3} M/10^{-4} M]$_0$; B) [C153/NR: 10^{-4}/10^{-4} M]$_0$ and C) [C153/NR:10^{-5} M/10^{-4} M]$_0$. *Second row* **(D-F)**, Group 2 composites, D) [C153/NR: 10^{-3} M/10^{-5} M]$_0$; E) [C153/NR: 10^{-4} M/10^{-5} M]$_0$ and F) [C153/NR:10^{-5} M/10^{-5} M]$_0$. (absorption (blue) and emission (red), excitation (emission at C153 maxima; green) and excitation (emission at NR maxima; black) spectra.

Energy transfer efficiency (ET) calculation: Efficient white light (WL) generation from a composite containing multiple chromophores requires energy transfer (ET) from the excited state of one dye to another, thereby enabling sequential excitation and emission across the visible spectrum. To achieve efficient WL it is essential to determine the efficiency of the ET process.

The emission from Group 2 composites is closer to WL, whereas for Group 1 composites the emission predominantly originates from the acceptor dye (NR). To quantify the efficiency of ET, we evaluated the ET from the donor dye (C153) to the acceptor dye (NR) using one representative composite from each group, both containing the same concentration of C153. We selected the $[C153/NR]_0$ composite with a C153 initial concentration of 10^{-4} M. The 10^{-5} M $[C153]_0$ composites were excluded based on the TCSPC measurements due to their extremely low fluorescence intensity, while the 10^{-3} M $[C153]_0$ composites exhibited fluorescence quenching caused by dye aggregation.

To calculate the ET efficiency from C153 to NR we used the Eq 1.

$$E = 1 - \frac{Q_{DA}}{Q_D} \qquad (1)$$

where E is the efficiency of ET, Q_{DA} and Q_D are the quantum yields of the donor (C153) in presence and absence of the acceptor (NR), respectively.

For the [C153/NR] composites, the emission region of C153 is selectively used to calculate the Q_{DA} to avoid the contribution from emission from NR in Q_{DA}. The emission range of 440 to 600 nm has been chosen to calculate the Q_D and Q_{DA}. The obtained Q_D for the $[10^{-4}\ M]_0$ of C153 composites is 22%, the Q_{DA} is 0.67% for the $[C153/NR{:}10^{-4}\ M/10^{-4}\ M]_0$ and 9.7% for $[C153/NR{:}10^{-4}\ M/10^{-5}\ M]_0$. We obtained an ET efficiency of

97% for the [C153/NR:10^{-4} M/10^{-4} M]$_0$ and 57% for the [C153/NR:10^{-4} M/10^{-5} M]$_0$ composites by using the Q_{DA} and Q_D values in Eq. 1.

The overall QY is calculated using the complete emission range from 440 nm to 800 nm. We obtained 23% QY for the [10^{-4} M]$_0$ of C153 composite, 4.1% for the [C153/NR:10^{-4} M/10^{-4} M]$_0$ and 13.3% for the [C153/NR:10^{-4} M/10^{-5} M]$_0$ composites. From these results it is evident that the final QY is higher for the lower initial concentration of the acceptor dye ([C153/NR:10^{-4} M/10^{-5} M]$_0$) compared to the more concentrated acceptor dye ([C153/NR:10^{-4} M/10^{-4} M]$_0$) which is explained in terms of aggregation induced quenching in the more concentrated composites.

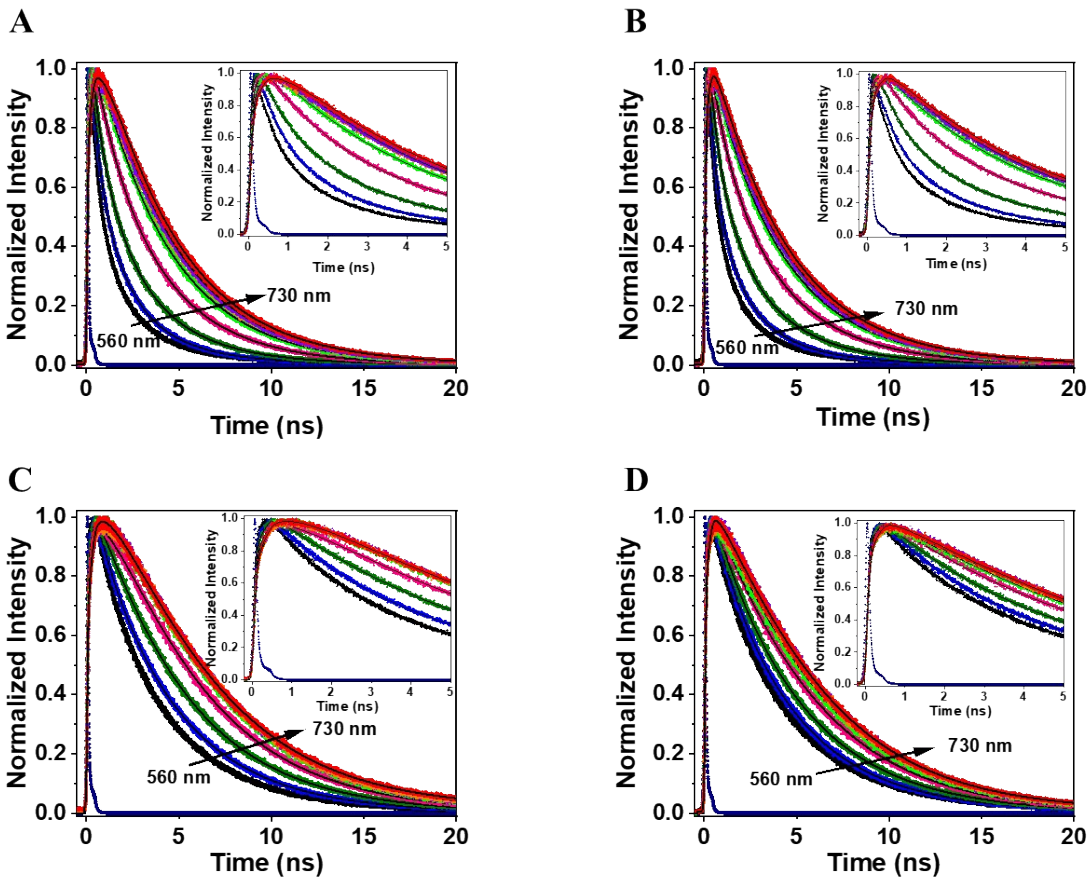

Figure S7. Emission decays (solid circles) of [NR/C153@Al-ITQ-HB] composites prepared using **A)** [C153/NR: 10^{-3} M/10^{-4} M]$_0$; **B)** [C153/NR: 10^{-4} M/10^{-4} M]$_0$; **C)** [C153/NR: 10^{-3} M/10^{-5} M]$_0$; and **D)** [C153/NR: 10^{-4} M/10^{-5} M]$_0$ collected at discrete wavelengths (560, 590, 630, 650, 680, 700 and 730 nm) following excitation at 505 nm. The solid lines (black) represent the best fits using multiexponential function. The dotted line is the measured instrument response function (IRF~ 70 ps; violet). The inset shows the decays up to 5 ns.

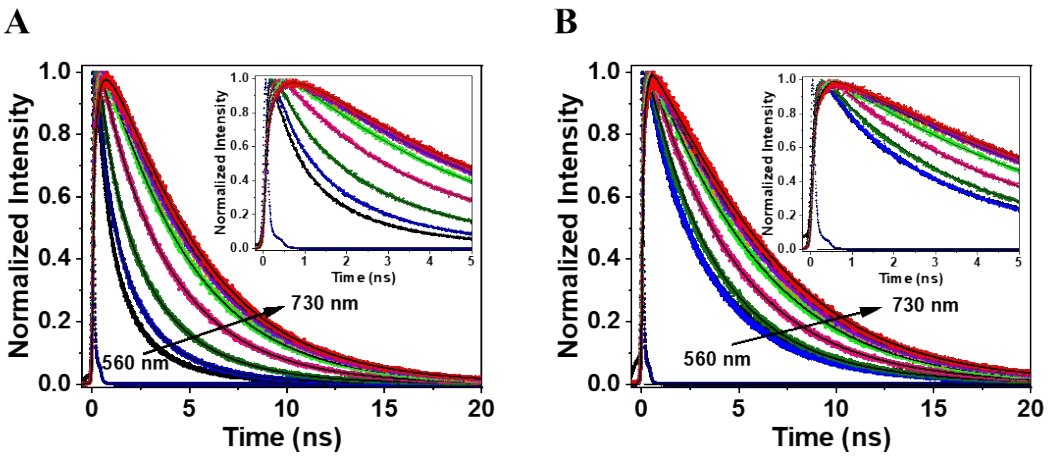

Figure S8. Emission decays (solid circles) of [C153/NR@Al-ITQ-HB] composites prepared using **A)** [C153/NR: 10^{-5} M/10^{-4} M]$_0$ and **B)** [C153/NR: 10^{-5} M/10^{-5} M]$_0$ collected at discrete wavelengths (in nm: 560, 590, 630, 650, 680, 700 and 730) following excitation at 505 nm. The solid lines represent the best fits using multiexponential function. The dotted line is the measured instrument response function (IRF~ 70 ps; violet). The insets show the zoomed decay plot up to 5 ns,.

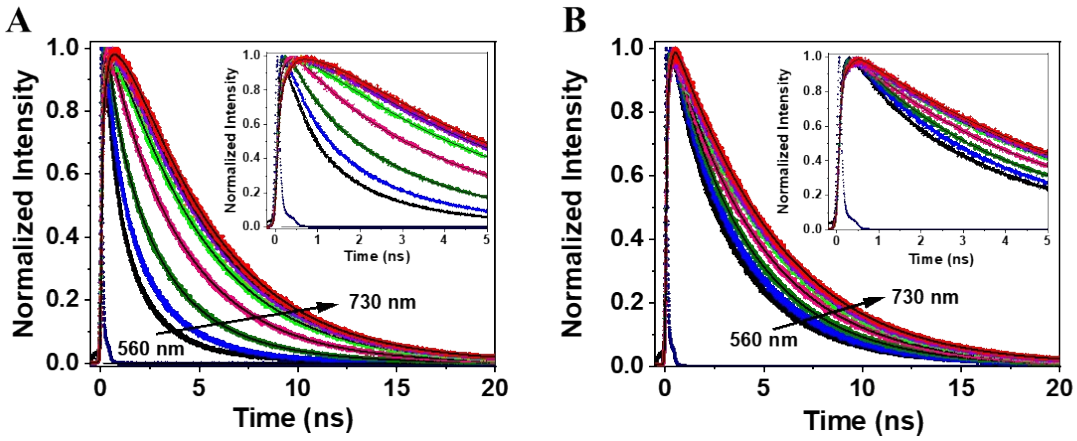

Figure S9. Emission decays (solid circles) of NR@Al-ITQ-HB composites prepared using **A)** 10^{-4} M and **B)** 10^{-5} M $[NR]_0$ collected at discrete wavelengths (in nm: 560, 590, 630, 650, 680, 700 and 730) following excitation at 505 nm. The solid lines (black) represent the best fits using multiexponential function. The dotted line is the measured instrument response function (IRF~ 70 ps; violet). The insets show the decay plot up to 5 ns.

Table S4. Values of the time components (τ_i), normalized (to 100) pre-exponential factors (A_i) and contributions (C_i), obtained by the multiexponential fit of different emission wavelength following excitation at 505 nm. A) [C153/NR: 10^{-3} M/10^{-4} M]$_0$; B) [C153/NR: 10^{-4} M/10^{-4} M]$_0$.

A)	**[C153/NR: 10^{-3} M/10^{-4} M]$_0$**									**B)**	**[C153/NR: 10^{-4} M/10^{-4} M]$_0$**							
λ_{obs} (nm)	τ_1 (ns)	A_1 (%)	C_1 (%)	τ_2 (ns)	A_2 (%)	C_2 (%)	τ_3 (ns)	A_3 (%)	C_3 (%)	τ_1 (ns)	A_1 (%)	C_1 (%)	τ_2 (ns)	A_2 (%)	C_2 (%)	τ_3 (ns)	A_3 (%)	C_3 (%)
560	0.4	50	12	2.1	35	50	4.0	15	48	0.3	59	18	1.8	33	54	4.1	7	27
590	0.4	36	7	2.1	37	32	4.0	27	61	0.3	49	12	1.8	51	51	4.1	12	35
610	0.4	23	4	2.1	36	25	4.0	41	71	0.3	35	6	1.8	37	21.2	4.1	25	56
630	0.4	-90	-90	2.1	-10	-10	4.0	100	100	0.3	-95	-95	1.8	-5	-5	4.1	100	100
650	0.4	-87	-87	2.1	-13	-13	4.2	100	100	0.3	-92	-92	1.8	-8	-8	4.1	100	100
680	0.4	-84	-84	2.1	-16	-16	4.2	100	100	0.3	-90	-90	1.8	-10	-10	4.1	100	100
700	0.4	-70	-70	2.1	-30	-30	4.2	100	100	0.3	-87	-87	1.8	-13	-13	4.1	100	100
730	0.4	-60	-60	2.1	-40	-40	4.2	100	100	0.3	-78	-78	1.8	-22	-22	4.1	100	100

Table S5. Values of the time components (τ_i), normalized (to 100) pre-exponential factors (A_i) and contributions (C_i), obtained by the multiexponential fit of different emission wavelength following excitation at 505 nm, A) [C153/NR: 10^{-5} M/10^{-4} M]$_0$; B) [C153/NR: 10^{-5} M/10^{-5} M]$_0$.

A)	**[C153/NR: 10^{-5} M/10^{-4} M]$_0$**									**B)**	**[C153/NR: 10^{-5} M/10^{-5} M]$_0$**							
λ_{obs} (nm)	τ_1 (ns)	A_1 (%)	C_1 (%)	τ_2 (ns)	A_2 (%)	C_2 (%)	τ_3 (ns)	A_3 (%)	C_3 (%)	τ_1 (ns)	A_1 (%)	C_1 (%)	τ_2 (ns)	A_2 (%)	C_2 (%)	τ_3 (ns)	A_3 (%)	C_3 (%)
560	0.3	38	5	2.0	32	45	4.2	30	50	0.3	49	10	2.4	28	50	4.6	51	40
590	0.3	34	3	2.0	30	28	4.2	36	69	0.3	39	4	2.4	41	30	4.6	66	55
610	0.3	22.6	2.7	2.0	31.7	21.0	4.2	45.6	76.2	0.3	19.3	1.9	2.4	31.6	23.8	4.6	49.0	74.2
630	0.3	1.2	0.1	2.0	11.6	4.6	4.2	87.3	95.3	0.3	0.25	3.6	2.4	-100	-100	4.6	9.75	96.4
650	0.3	-29	-29	2.0	-71	-71	4.2	100	100	0.3	-17	-17	2.4	-87	-87	4.6	100	100
680	0.3	-20	-20	2.0	-80	-80	4.2	100	100	0.3	-15	-15	2.4	-85	-85	4.6	100	100
700	0.3	-21	-21	2.0	-79	-79	4.2	100	100	0.3	-12	-12	2.4	-88	-88	4.6	100	100
730	0.3	-24	-24	2.0	-76	-76	4.2	100	100	0.3	-10	-10	2.4	-80	-80	4.6	100	100

Table S6. Values of the time components (τ_i), normalized (to 100) pre-exponential factors (A_i) and contributions (C_i), obtained by the multiexponential fit of different emission wavelength following excitation at 505 nm. A) 10^{-4} M; B) 10^{-5} M of $[NR]_0$.

A)	**10^{-4} M $[NR]_0$**									**B)**	**10^{-5} M $[NR]_0$**							
λ_{obs} (nm)	**τ_1 (ns)**	**A_1 (%)**	**C_1 (%)**	**τ_2 (ns)**	**A_2 (%)**	**C_2 (%)**	**τ_3 (ns)**	**A_3 (%)**	**C_3 (%)**	**τ_1 (ns)**	**A_1 (%)**	**C_1 (%)**	**τ_2 (ns)**	**A_2 (%)**	**C_2 (%)**	**τ_3 (ns)**	**A_3 (%)**	**C_3 (%)**
560	**0.32**	**8.8**	**12.5**	**1.8**	**44.8**	**57.8**	**4.2**	**46.7**	**29.6**	**0.35**	**16.7**	**2.1**	**2.0**	**54.5**	**52.5**	**4.5**	**28.7**	**45.4**
590	**0.32**	**32.3**	**5.2**	**1.8**	**37.7**	**31.7**	**4.2**	**29.8**	**63.0**	**0.35**	**12.1**	**1.0**	**2.0**	**21.4**	**15.6**	**4.5**	**66.5**	**83.4**
610	**0.32**	**21.7**	**2.4**	**1.8**	**30.1**	**19.9**	**4.2**	**48.2**	**77.6**	**0.35**	**8.4**	**0.7**	**2.0**	**14.7**	**10.6**	**4.5**	**76.8**	**88.6**
630	**0.32**	**5.0**	**1.0**	**1.8**	**21.0**	**15.0**	**4.2**	**73.0**	**83.0**	**0.35**	**3.9**	**0.3**	**2.0**	**-100**	**-100**	**4.5**	**96.1**	**99.7**
650	**0.32**	**-29**	**-29**	**1.8**	**-71**	**-71**	**4.2**	**100**	**100**	**-**	**-**	**-**	**2.0**	**-100**	**-100**	**4.5**	**100**	**100**
680	**0.32**	**-21**	**-21**	**1.8**	**-79**	**-79**	**4.2**	**100**	**100**	**-**	**-**	**-**	**2.0**	**-100**	**-100**	**4.5**	**100**	**100**
700	**0.32**	**-22**	**-22**	**1.8**	**-78**	**-78**	**4.2**	**100**	**100**	**-**	**-**	**-**	**2.0**	**-100**	**-100**	**4.5**	**100**	**100**
730	**0.32**	**-23**	**-23**	**1.8**	**-77**	**-77**	**4.2**	**100**	**100**	**-**	**-**	**-**	**2.0**	**-100**	**-100**	**4.5**	**100**	**100**

Table S7. Values of the time components (τ_i), normalized (to 100) pre-exponential factors (A_i) and contributions (C_i), obtained by the multiexponential fit of different emission wavelength following excitation at 505 nm. A) [C153/NR: $10^{-3}/10^{-5}$ M]$_0$; B) [C153/NR: 10^{-4} M/10^{-5} M]$_0$.

A)	**[C153/NR: 10^{-3} M/10^{-5} M]$_0$**									**B)**	**[C153/NR: 10^{-4} M/10^{-5} M]$_0$**							
λ_{obs} (nm)	**τ_1 (ns)**	**A_1 (%)**	**C_1 (%)**	**τ_2 (ns)**	**A_2 (%)**	**C_2 (%)**	**τ_3 (ns)**	**A_3 (%)**	**C_3 (%)**	**τ_1 (ns)**	**A_1 (%)**	**C_1 (%)**	**τ_2 (ns)**	**A_2 (%)**	**C_2 (%)**	**τ_3 (ns)**	**A_3 (%)**	**C_3 (%)**
560	**0.5**	**13**	**2**	**2.4**	**44**	**38**	**4.8**	**42**	**60**	**0.45**	**11**	**3**	**2.2**	**35**	**24**	**4.8**	**54**	**73**
590	**0.5**	**19**	**3**	**2.4**	**41**	**37**	**4.8**	**40**	**59**	**0.45**	**4**	**2**	**2.2**	**33**	**21**	**4.8**	**63**	**77**
610	**0.5**	**3**	**5**	**2.4**	**27**	**17**	**4.8**	**70**	**78**	**0.45**	**2**	**1**	**2.2**	**11**	**7**	**4.8**	**87**	**92**
630	**0.5**	**-44**	**-44**	**2.4**	**-56**	**-56**	**4.8**	**100**	**100**	**0.45**	**-100**	**-100**	**2.2**	**8**	**5**	**4.8**	**92**	**95**
650	**0.5**	**-20**	**-20**	**2.4**	**-80**	**-80**	**4.8**	**100**	**100**	**0.45**	**-14**	**-14**	**2.2**	**-86**	**-86**	**4.8**	**100**	**100**
680	**0.5**	**-17**	**-17**	**2.4**	**-83**	**-83**	**4.8**	**100**	**100**	**0.45**	**-13**	**-13**	**2.2**	**-87**	**-87**	**4.8**	**100**	**100**
700	**0.5**	**-15**	**-15**	**2.4**	**-85**	**-85**	**4.8**	**100**	**100**	**0.45**	**-12**	**-12**	**2.2**	**-88**	**-88**	**4.8**	**100**	**100**
730	**0.5**	**-14**	**-14**	**2.4**	**-86**	**-86**	**4.8**	**100**	**100**	**0.45**	**-11**	**-11**	**2.2**	**-89**	**-89**	**4.8**	**100**	**100**

Effect of Preparation Method, Central Metal and Ligand Chain length on Energy Transfer (ET)

Synthesis: To investigate the impact of the dye loading sequence on the ET behavior in MOF composites, two sequential methods of preparation were explored using the Al-ITQ-HB framework. In Method 1, a 10^{-4} M $[C153]_0$ solution in DCM was first added to 50 mg of Al-ITQ-HB MOF. This mixture was stirred continuously for 24 hours to ensure thorough incorporation of C153 into the porous framework. Next, the solvent was allowed to evaporate at room temperature, resulting in the formation of the C153@Al-ITQ-HB MOF composite. Then, a 10^{-5} M $[NR]_0$ solution in DCM was added, and the mixture was stirred and evaporated, yielding the final mixed composite [C153/NR: 10^{-4} M/10^{-5} M]$_0$. In Method 2, the sequence of dye incorporation was reversed. Here, first we add 10^{-5} M $[NR]_0$ solution to the 50 mg of Al-ITQ-HB and stirred under the same conditions, followed by solvent evaporation. Then the 10^{-4} M $[C153]_0$ solution was added to the resulting NR@Al-ITQ-HB composite and following the same procedure as in Method 1, to obtain the mixed dye composite.

References

(1) García-García, P.; Moreno, J. M.; Díaz, U.; Bruix, M.; Corma, A. Organic–inorganic supramolecular solid catalyst boosts organic reactions in water. *Nature Communications* **2016**, *7* (1), 10835.
(2) Caballero-Mancebo, E.; Moreno, J. M. a.; Corma, A.; Diaz, U.; Cohen, B.; Douhal, A. How does the surface of Al–ITQ-HB 2D-MOF condition the intermolecular interactions of an adsorbed organic molecule? *ACS Applied Materials & Interfaces* **2018**, *10* (23), 20159-20169.
(3) Organero, J.; Tormo, L.; Douhal, A. Caging ultrafast proton transfer and twisting motion of 1-hydroxy-2-acetonaphthone. *Chemical physics letters* **2002**, *363* (3-4), 409-414.
(4) Gomez, E.; Gutiérrez, M.; Cohen, B.; Hisaki, I.; Douhal, A. Single crystal fluorescence behavior of a new HOF material: a potential candidate for a new LED. *Journal of Materials Chemistry C* **2018**, *6* (26), 6929-6939.